Numerical Simulation of Gel Electrophoresis of DNA Knots in Weak and Strong Electric Fields

C. Weber,* A. Stasiak,† P. De Los Rios,‡ and G. Dietler§

*Institut Romand de Recherche Numérique en Physique des Matériaux (IRRMA), Ecole Polytechnique Fédérale de Lausanne (EPFL), CH-1015 Lausanne, Switzerland; †Laboratoire d'Analyse Ultrastructurale (LAU), Université de Lausanne, CH-1015 Lausanne, Switzerland; ‡Institut de Physique Théorique, EPFL, CH-1015 Lausanne, Switzerland; and §Laboratoire de Physique de la Matière Vivante, EPFL, CH-1015 Lausanne, Switzerland

ABSTRACT Gel electrophoresis allows one to separate knotted DNA (nicked circular) of equal length according to the knot type. At low electric fields, complex knots, being more compact, drift faster than simpler knots. Recent experiments have shown that the drift velocity dependence on the knot type is inverted when changing from low to high electric fields. We present a computer simulation on a lattice of a closed, knotted, charged DNA chain drifting in an external electric field in a topologically restricted medium. Using a Monte Carlo algorithm, the dependence of the electrophoretic migration of the DNA molecules on the knot type and on the electric field intensity is investigated. The results are in qualitative and quantitative agreement with electrophoretic experiments done under conditions of low and high electric fields.

INTRODUCTION

Gel electrophoresis of linear and circular DNA and its dynamics has long been subject of numerical simulations and analytical approaches (1–8).

Most experimental and theoretical studies of the electrophoresis process deal with linear or circular DNA (9–12). But DNA comes also in knotted forms. Various classes of enzymes (topoisomerases and site-specific recombination enzymes) produce different types of knots or catenanes by acting on circular DNA molecules (13,14). The analysis of these knots provides important information about the mechanisms of action of these enzymes that are involved in the proper functioning of chromosomes (see, for example, Duplantier et al. (15) and Schvartzman and Stasiak (16)). Knots also arise as a result of DNA packing in phage heads; analysis of these knots sheds light on the arrangement of DNA in the tightly packed state (17). Being able to study knots produced by a given enzyme in prescribed conditions implies being able to perform some sort of ''knot spectroscopy'' that can be done, for example, by electron microscopy, where knots are observed one by one. Yet, if large numbers of knots need to be classified, then some high throughput technique is needed. Such a technique is gel electrophoresis. Indeed, experimental work has shown a linear relationship between the distance of electrophoretic migration on agarose gel of different types of DNA knots (all with the same number of basepairs) and the average crossing number of the ideal geometrical representations of the corresponding knots (closely related to the complexity of the knot) (18). As a consequence, the type of a knot can be simply identified by measuring its position on the gel, without the need of electron microscopy experiments as required until recently. An exception to this rule concerns right- and left-handed forms of the same knot that cannot, generally, be distinguished by gel electrophoresis.

At low electric field, the usual observation is that the more complex the knot is, the higher is its mobility. A simple intuitive explanation for this behavior is that the compactness of a knot increases with its complexity (for a constant string length) and the friction coefficient $\gamma = 6\pi\eta_0 R_H$ (with R_H the hydrodynamic radius of the knot and η_0 the viscosity of the solvent) is smaller, resulting in higher mobilities. A more refined calculation of the friction coefficient γ relies on the Kirkwood-Riseman formula (19)

$$\gamma_{KR} = \left(\sum_{i=1}^{N}\zeta_i\right)\left[1 + \left(6\pi\eta_0\sum_{i=1}^{N}\zeta_i\right)^{-1}\sum_{i=1}^{N}\sum_{j=1}^{N}\zeta_i\zeta_j R_{ij}^{-1}\right]^{-1}, \quad (1)$$

where the chain is modeled by N beads of radius σ_i and friction coefficient $\zeta_i = 6\pi\eta_o\sigma_i$, and R_{ij} is the distance between beads i and j. The term $(1/R_{ij})$, due to hydrodynamic interactions between beads, in the second factor of Eq. 1 explains the observed behavior: more compact molecules have smaller distances R_{ij}, and thus a smaller friction coefficient. The calculations of an average friction coefficient $\bar{\gamma}_{KR}$ for an equilibrium set of thermally agitated DNA molecules forming different types of knots agree with the experimental results (20).

Recently, it was observed by two-dimensional agarose gel electrophoresis that when the strength of the electric field is increased, the electrophoretic mobility of DNA knots changes behavior (Fig. 1) (21,22). Two-dimensional gels are run in two steps: a low strength electric field of 0.6–1 Vcm^{-1} is first applied along one direction in the gel. At this step, more complex knots show a higher mobility, in agreement with the Kirkwood-Riseman formula. During a second step, a stronger electric field (~5 Vcm^{-1}) is applied perpendicularly to the

Submitted July 21, 2005, and accepted for publication January 12, 2006.

Address reprint requests to Giovanni Dietler, E-mail, giovanni.dietler@epfl.ch.

0006-3495/06/05/3100/06 $2.00

doi: 10.1529/biophysj.105.070128

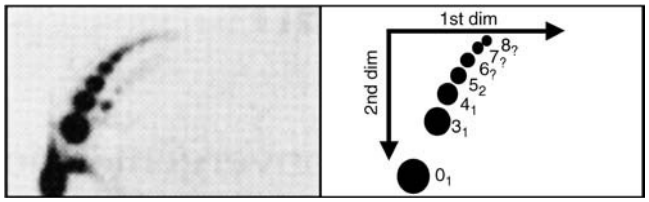

FIGURE 1 Separation of knotted DNA molecules of the same size by two-dimensional agarose gel electrophoresis (*left*, autoradiogram of the gel; *right*, diagrammatic interpretation). It is visible that at low voltage conditions (first dimension, 1 Vcm^{-1}), the more complex knots migrate quicker than simpler knots, whereas the opposite is the case for high strength of electric field (second dimension, 5 Vcm^{-1}). Reproduced from Sogo et al. (22) with permission.

first one. In this case, the opposite behavior is observed: more complex knots cover smaller distances than simple ones.

The presence of two regimes of weak and strong electric field can be captured with a simple argument. A knot of size ξ drifts over a distance equal to its size along the direction of the applied electric field $\mathcal{E}$ in a time $t_\xi \simeq \xi/v = \gamma_{KR}\xi/q\mathcal{E}$, where $v = q\mathcal{E}/\gamma_{KR}$ is the drift velocity in the stationary regime and q the total electrical charge carried by the DNA molecule. During the same time, the drifting knot diffuses laterally over a distance $d \simeq \sqrt{2Dt_\xi} = \sqrt{2(k_BT/\gamma_{KR})t_\xi} = \sqrt{2(k_BT/q\mathcal{E})\xi}$, where T is the absolute temperature and k_B is the Boltzmann's constant. If the transverse diffusion explores distances d much larger than the typical size of the knot, ξ, then, on average, the knot will be deflected by the gel fiber and the knots will drift with a slight renormalization of the friction coefficient. If instead $d \ll \xi$, then whenever a knot is on a collision course with a gel strand, it can be trapped by the fiber. As a consequence, after being trapped at the obstacle, the knot needs to crawl around it to free itself. Crawling around an obstacle is much more difficult for more complex knots than for simple ones, due to the self-avoidance constraint. Following this argument, the two electric field regimes are separated by a critical field $\mathcal{E}_c$ that can be obtained by setting $d \simeq \xi$, giving $\mathcal{E}_c \simeq 2(k_BT/q\xi)$. To estimate $\mathcal{E}_c$, we use the typical values for an 11,000 basepairs DNA knot: the size of a closed DNA ring is about $\xi = 300$ nm; this value is estimated from atomic force microscope images of complex knots (23). The knots were kindly provided by Dr. J. Roca (IBMB, CID-CSIC, Barcelona, Spain) and the atomic force microscope images were taken by Dr. F. Valle (LPMV, EPFL, Lausanne, Switzerland). The total charge q depends on the gel conditions, since every nucleotide carries a P^- group, hence one electron negative charge, which can be strongly screened by charges in the solvent. As a consequence, we use $q \sim 10^{-15}$–10^{-16} C. We then obtain a critical field $\mathcal{E}_c = 0.1 - 1\,Vcm^{-1}$ in reasonable agreement with experiments (21,22). The expression for the critical electric field holds also in the case when the gel is concentrated, as it is the case in many experiments. Under the condition of high gel density, the DNA is filling the pores, and the expression for the collision condition is that the DNA lying between two gel strands will collide with one gel strand before the DNA can drift transversally to the direction of the electric field. Instead of ξ, one has to insert the gel pore size ℓ. The lateral diffusion constant D^* has to be rescaled to include the effect of the gel. The condition for the critical electric field reads again $\mathcal{E}_c \simeq 2(k_BT/q\ell)$.

One has also to note that the two conditions for the critical electric field $\mathcal{E}_c$ actually mean that the energy gained by the DNA when moving one diameter ξ or one pore size ℓ along the electric field is twice the thermal energy: $q\mathcal{E}_c\xi$ (or ℓ) $\simeq 2\,k_BT$. Although the above model gives a first hint of the origin of the observed behavior, here we want to address the issue more thoroughly using lattice Monte Carlo simulations.

Lattice Monte Carlo simulations are widely used in biophysical studies aimed to grasp basic principles of such complex phenomena as protein folding (24) or polymer knotting (25). Most frequently, a simple cubic lattice is applied where any point of the lattice cannot be visited more than once. Although standard simulations on such a cubic lattice are not precise enough to model fine structural aspects like, for example, the effect of varying excluded volume on the structure of modeled polymers, this simulation procedure reproduces perfectly scaling properties of self-avoiding polymers and gives the scaling exponent $\nu = 0.588$ in practically the same way as in off-lattice models where the effective diameter can be easily varied (26,27). Also, investigations of random knotted polygons of a given type revealed that their writhe (a measure of chirality) is the same for random polygons on a cubic lattice and random polygons off lattice, although the latter ones were modeled as very thin chains (28,29). This demonstrates that lattice models are very valuable for grasping essential phenomena such as scaling of self-avoiding polymers or their topological properties.

Our study is not intended to model the exact conformation of DNA molecules in the gel nor the exact shape of gel fibers. Our aim is to grasp the basic principles of the inversion of gel mobility of DNA knots upon the increase of the field intensity.

METHODS

DNA knots are modeled by closed self-avoiding walks composed of N segments of length a on a three-dimensional cubic lattice (the lattice constant a is comparable to the persistence length of the DNA molecules). The gel is a two-dimensional grid forming a sublattice with a mesh size b (equal to the gel parameter) and perpendicular to the applied electric field (so that no knots can ever get impaled). The gel lattice is shifted by the quantity $(\frac{a}{2}, \frac{a}{2}, \frac{a}{2})$ compared to the knot lattice, so that no points of the knot lie on the gel. Knots are not allowed to cross the gel network. The coordinates of the N monomers in the configuration at time t are written as

$$\bar{r}(t) = (\vec{r}_1(t), \vec{r}_2(t), \ldots, \vec{r}_N(t)) \quad (2)$$

with constraints $\| \vec{r}_j(t) - \vec{r}_{j+1}(t) \| = a$.

The dynamics is followed using the Berg-Foerster-Aragao de Carvalho-Caracciolo-Froehlich (BFACF) algorithm (30–32). Two types of moves are allowed: a), the creation/destruction of a handle, and b), the flip of a corner into the mirror position (see Fig. 2). The first move clearly does not preserve the knot length, which can vary by ± 2 at every step, but introduces the knot

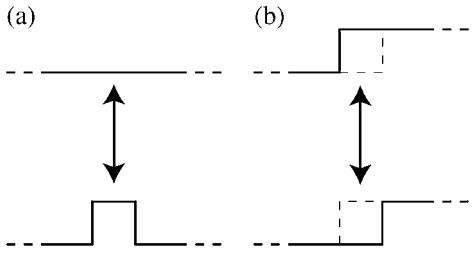

FIGURE 2 Elementary moves of the BFACF algorithm. (*a*) Creation/destruction of a handle, and (*b*) corner flip.

elasticity. The BFACF algorithm preserves knot classes, within which it is ergodic (33). Self-avoidance is imposed by disallowing monomers to visit any site that is already occupied by other monomers. Furthermore, knots are not allowed to cross gel rods, so that corner flips and handle creation/destruction are forbidden when a rod has to be crossed.

Under an external uniform electric field $\vec{\varepsilon}$, the electrostatic energy at time t is given by

$$E_q(t) = -\frac{q}{N(t)}\sum_{j=1}^{N}\vec{r}_j(t)\ \cdot\ \vec{\varepsilon}. \tag{3}$$

$N(t)$ is the length of the knot at time t, and it is associated with an elastic energy

$$E_{el}(t) = \frac{1}{2}K[N(t) - N_0]^2, \tag{4}$$

where K is the spring constant. In the simulation, a value $K/k_BT = 0.1$ was used. The knot energy is then $E(t) = E_q(t) + E_{el}(t)$.

At each time step, we choose a point at random on the chain and propose alternatively one of the two moves. If it satisfies the self-avoiding and gel-avoiding constraints, it is accepted with a probability given by the Metropolis algorithm: if the energy of the new trial configuration, E_{trial}, is lower than that of the previous configuration, $E_{old} = E(t)$, the move is accepted and $\bar{r}(t+1) = \bar{r}_{trial}$; otherwise, the probability of acceptance of the trial configuration is equal to $\exp\{-[E_{trial} - E(t)]\}/k_BT$. If the move is rejected, then $\bar{r}(t+1) = \bar{r}(t)$.

We used a set of 100 trial initial knot configurations, for each different knot type consisting of 150 segments drawn manually on the cubic lattice (without distinction of chirality). Simulations were done for each of these starting trial configurations, and then the data were averaged over all starting knot configurations. The Alexander polynomial (34) was calculated to check that the knot type did not change during the simulation. Starting from the trial knot configuration, we let the system freely relax to thermodynamic equilibrium in the absence of an external field ($\mathcal{E} = 0$) until correlations from the initial configuration have disappeared. Then the electric field is switched on, and we let the knots migrate in the gel. The computed quantities are the position of the center-of-mass and the average crossing number (ACN) of the knot along a trajectory.

Time is measured in Monte Carlo iterations, length in lattice spacing. The initial length N_0 of our polymers was set to 150, and the mean length of the knot depends generally on the electric field and on the gel parameter. However, the mean length is 145 (146) for $C = 0.1$ ($C = 0.4$) and $b = 20$, and we checked that during the simulations it fluctuates around that value. The average length is slightly shorter that N_0, since the probability of shortening the polymer is a slightly larger than the probability of lengthening it due to the self-avoiding condition. The gel parameter was set to $b = 20$ (in units of a), corresponding to a relatively sparse gel with big pores. For each initial knot, 20×10^6 iterations were performed. The center-of-mass position has been measured every 1000 Monte Carlo steps, and it was then averaged over the trajectories obtained by the migration of 100 different initial knots.

One feature of the Monte Carlo algorithm is that more complex knots have a smaller drift velocity than less complex ones even in the absence of the gel, when time is measured in Monte Carlo steps. This is due to the fact that already in the absence of the gel, the number of rejected moves is proportional to the complexity of the knot, due to the self-avoidance condition. Therefore,

$$v(ACN) = \frac{q\epsilon}{\gamma(ACN)}, \tag{5}$$

where $\gamma(ACN)$ is an internal friction coefficient related to the Monte Carlo algorithm that depends on the average crossing number of the knots. To find the relation between the real time (t_R) and the number of Monte Carlo steps (t_{MC}), we used the Kirkwood-Riseman formula (1) to compute the relation between the friction coefficient γ_{KR} and the ACN of the different knots.

Imposing $\gamma(ACN) = \gamma_{KR}(ACN)$ gives a relation between the real time and the number of Monte Carlo steps, $t_{MC} = F(ACN) \times t_R$. Interestingly enough, we find that F is a linear function of the ACN such that $t_{MC}/t_R = F(ACN) = \alpha \times ACN - \beta$, finding $\alpha = 0.067(1)$ and $\beta = 0.993(1)$. However, for a given knot, the collision of the knot with the gel will make it more elongated along the electric field direction, and therefore its geometry will be anisotropic. Since the mean cross section, which is responsible for the Kirkwood drag, will be smaller due to this deformation, we correct slightly the time rescaling by multiplying it with the following geometry factor: $t_{MC}/t_R = F(ACN_{free}) \times (R_{gel}/R_{free}) \approx (F(ACN_{free})^2/F(ACN_{gel}))$, where R_{free} (R_{gel}) is the mean radius of gyration in the free solution (gel), and ACN_{free} (ACN_{gel}) is the mean ACN of the knot moving along a trajectory in the free solution (gel).

RESULTS AND DISCUSSION

To test our algorithm, we have considered first the case when there is no electric field. The knot is expected to move randomly through the gel, and the center-of-mass should therefore follow a simple diffusive random walk, which is nicely confirmed by the simulation results (see Fig. 3).

Fig. 4 presents how the simulated migration speed changes with the strength of the electric field (represented by the dimensionless parameter $\mathcal{C} = q\mathcal{E}a/k_BT$) in the case of linear DNA molecules and also for simple and complex DNA knots. The simulations performed for linear DNA molecules reveal

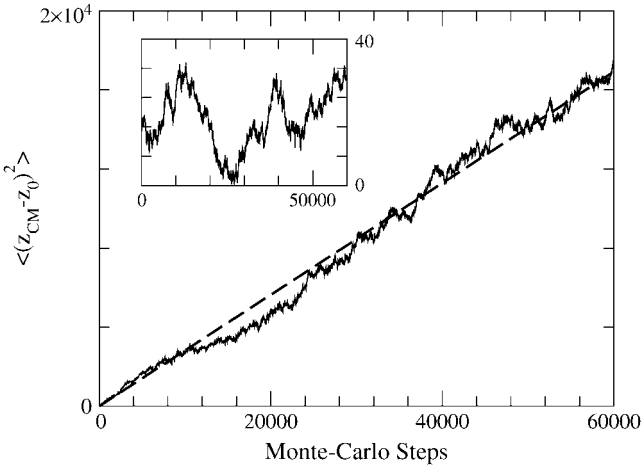

FIGURE 3 Mean-squared difference of the center-of-mass position at time t (z_{CM}) and its initial value at time $t = 0$ (z_0), averaged over 100 different simulations, when there is no electric field ($C = 0$). We find a linear relation, as expected for a diffusive Markovian random walk. The dashed line is a linear fit of the data. Time is measured here in units of the number of Monte Carlo steps. (*Inset*) Center-of-mass position versus the time for one specific simulation.

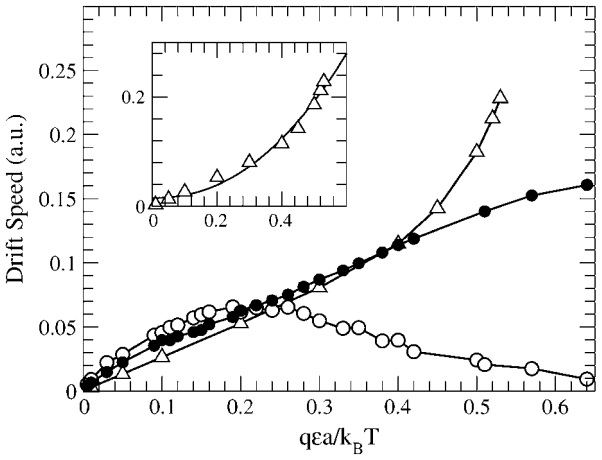

FIGURE 4 Drift velocity in arbitrary units for the 3_1 (●) and 8_1 (○) knots as function of $\mathcal{C} = q\mathcal{E}a/k_BT$. Also plotted is the drift velocity of the linear DNA (△). The lines are only guides for the eyes. (*Inset*) Quadratic fit of the drift velocity of the linear DNA.

that in the tested range of the electric field ($0 < C < 0.5$), the speed of electrophoretic migration v is well fitted with a quadratic dependence upon C: $v = aC^2 + b$, where b is a small offset that permits a better fit. These results are in agreement with experimental data (35).

In the case of knot 3_1, we observed that the increase of the electrophoretic speed becomes less pronounced starting from a strength of the electric field corresponding to about $C = 0.5$. More complex knots, like 8_1, for example, show a decrease of electrophoretic speed starting at about $C = 0.2$. Moreover, in our simulations for $C < 0.2$, the 8_1 knots migrate quicker than 3_1 knots, but for $C > 0.22$ the opposite is observed. This agrees with the actual gel electrophoresis experiments (see Fig. 1).

Fig. 5 presents the effect of strong and weak electric fields ($\mathcal{C} = 0.4$and $\mathcal{C} = 0.1$, respectively) on the migration speed of 11 types of knots (3_1, 4_1, 5_1, 5_2, 6_1, 6_2, 6_3, 7_1, 7_2, 7_3, and 8_1) all having a rest length of 150 monomers. For each knot type, we extract the average velocity from the distance of migration versus time curve. The velocity of migration is then plotted as a function of the measured ACN that is related to the knot type. This relation is presented in Fig. 5, *a* and *b*, for high and low electric fields, respectively. We observe that there is a fairly linear relationship between the average velocity of knots and the ACN (measure of complexity). More complex knots migrate slower than simpler ones at strong electric fields (although much noisier than for weak fields). These results are in agreement with experiments. The data for low electric field ($\mathcal{C} = 0.1$) are shown in Fig. 5 *b*. Table 1 summarizes the obtained results. We have also compared the average velocity of migration of different knots at low electric field in a free solution and in a gel (see Fig. 6). We conclude that at low electric field, the migration speed is only weakly affected by the gel, and the migration order of different knot types is the same in the two cases.

The intuitive view of a knot making its way through the pores of the gel would have as a consequence that more complex (thus more compact) knots migrate faster than simple knots, because they are less disturbed by the gel. This is indeed what happens in weak electric fields. In the strong field regime, our simulations are in agreement with experiments and show the opposite behavior, indicating that the migration of complex knots around the gel strands becomes more difficult. Somehow, parts of the knot have to go around other parts of itself, a process that is much longer for complex knots than for simple knots.

We must emphasize that our dynamic suffers from the fact that we consider only thermal activated processes for describing the knot going around an obstacle, which are known to have an exponentially long relaxation time (6,36). Yet, adding suitable nonlocal moves would be enough to eliminate the artificial slowing down of the dynamics due to our local

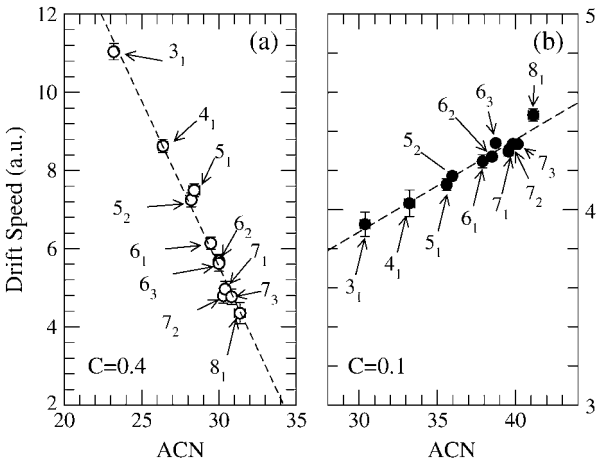

FIGURE 5 Linear relation between the electrophoretic drift velocity of the center-of-mass as a function of the average crossing number (determined during the simulation) for different knots at (*a*) high and (*b*) low electric fields.

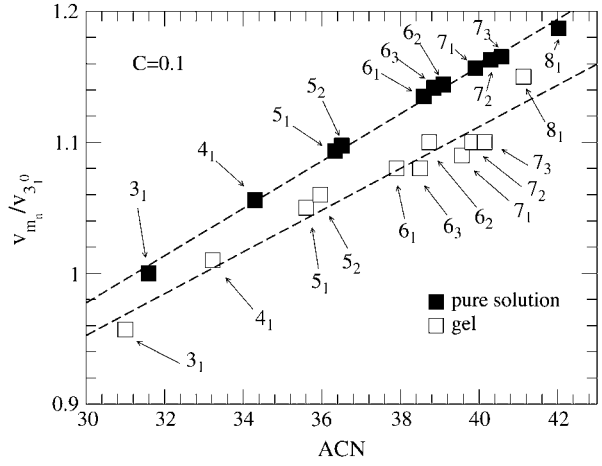

FIGURE 6 Electrophoretic drift velocity as a function of the average crossing number at low electric fields in free solution and in the gel, respectively. We normalized all the values by the speed of the knot 3_1 moving in the free solution ($v^0_{3_1}$).

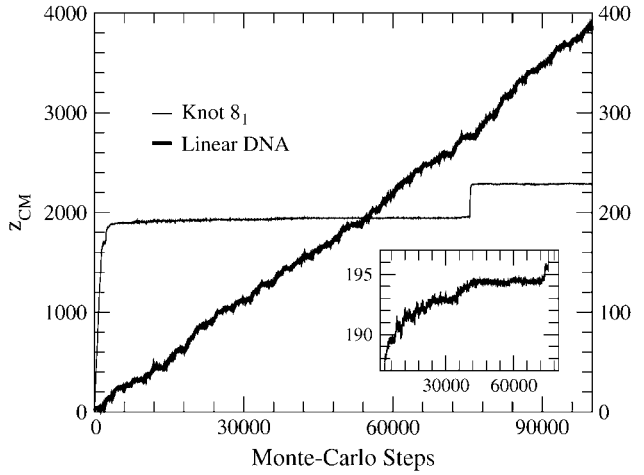

FIGURE 7 Position of the center-of-mass versus the number of Monte Carlo steps at high electric field ($C = 0.7$) for the 8.1 knot (*normal line*, *right scale*) and for the linear DNA (*bold line*, *left scale*). There is no appearance of large plateaus for the case of the linear DNA. (*Inset*) Zoom on the plateau for the 8.1 knot. The center-of-mass is moving slowly in the direction of the field; during this time the knot crawls around the gel rod.

TABLE 1 Drift velocity for the simulated data and experimental data for knots from 3_1 to 8_1

Knot type	v/v_{3_1}, low field	v/v_{3_1}, high field
Experiments		
4_1	1.01	0.78
5_2	1.05	0.64
$6_?$	1.07	0.52
$7_?$	1.09	0.43
$8_?$	1.12	0.37
Simulations		
4_1	1.02(1)	0.78(1)
5_1	1.05(1)	0.65(1)
5_2	1.06(1)	0.64(1)
6_1	1.08(1)	0.55(1)
6_2	1.09(1)	0.51(1)
6_3	1.10(1)	0.50(1)
7_1	1.08(1)	0.43(1)
7_2	1.09(1)	0.45(1)
7_3	1.10(1)	0.43(1)
8_1	1.14(2)	0.39(1)

Experimental data are from Sogo et al. (22). Simulation at low electric field ($\mathcal{E} = 0.6\,\mathrm{V/cm}$ and $\mathcal{C} = 0.1$, respectively) and for high electric field ($\mathcal{E} = 5\,\mathrm{V/cm}$ and $\mathcal{C} = 0.4$) are depicted. The values were all normalized to their respective value for the knot 3_1.

dynamic. However, the closed knot topology of DNA in our numerical simulations does not allow us to introduce the long range moves.

However, we argue that exponentially long relaxation times present in our simulations affect equally, in first approximation, all the knots, irrespective of their topology. In the ideal case of purely mechanical and frictionless unbinding, one can easily check that the knot complexity introduces at most a small logarithmic correction according to which more complex knots would anyway unpin faster, in contradiction with both experiments and our simulation. Therefore, the simulated absolute drift velocity v_{abs} is affected by a timescale that is artificially stretched in essentially the same way independent of the knot class. So, by looking at the ratios of the absolute velocities, this timescale should in first approximation cancel out.

In addition, we have tested our algorithm in the simple case of linear DNA molecules, to check that the plateaus induced in the knotted polymer dynamics aren't an artifact of the method. Indeed, no plateaus induced by any temporary trapped configurations of the linear polymers were found even at very high electric field $C = 0.7$ (see Fig. 7). Also, the quadratic behavior of the speed versus the electric field of the linear DNA match well the experiments (35). When a knot hits a gel rod, it is slowed down, because the probability of a backward step is very small, and it is a growing function of the temperature T. Crawling around a gel fiber introduces plateaus in the migration distance as a function of time for individual knots, hence reducing the average migration velocity.

In Table 1, we show the simulated and experimental ratios $v^{\mathrm{abs}}_{\mathrm{m_n}}/v^{\mathrm{abs}}_{3_1}$ for comparison. The question mark index in the experimental data (in $6_?$, for example) indicates that only the minimal crossing number of the analyzed knots was known. The agreement between experimental data and simulations is remarkable. We show a graphic interpretation of Table 1 in Fig. 8.

In weak electric field, the transport properties of DNA knots are dominated by the hydrodynamics of the knots, and the gel plays a minor role. At high electric fields, the knot-gel

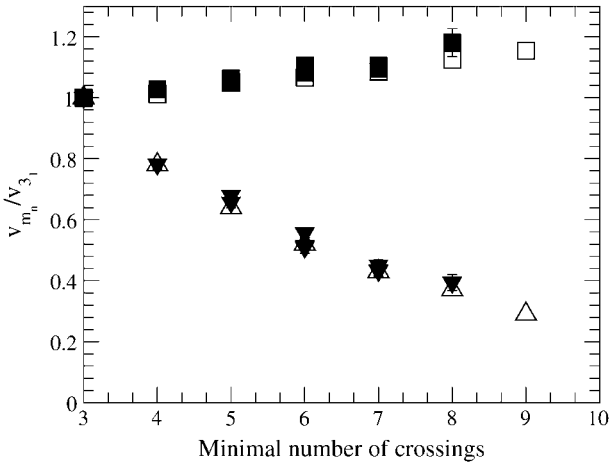

FIGURE 8 Simulated and experimental drift velocities versus the minimal number of crossings ranging from 3 to 9. The exact knot type in gel electrophoresis experiments is not determined beyond the minimal number of crossings. Therefore, we use this latter quantity rather than the usual ACN. Experimental data are from Sogo et al. (22). Squares are for low electric field ($\mathcal{E} = 0.6\,\mathrm{V/cm}$ and $\mathcal{C} = 0.1$, respectively) and triangles are for high electric field ($\mathcal{E} = 5\,\mathrm{V/cm}$ and $\mathcal{C} = 0.4$). Open symbols are the experimental results and solid symbols for the simulations results. The values were all normalized to their respective value for the knot 3_1.

interaction is predominant, and it is responsible for the inversion phenomenon. In particular, strong DNA-gel interactions enhance the effect of self-avoidance within the knotted DNA, and self-avoidance must be included in simulations to reproduce the correct behavior. This is at variance with simulations of gel electrophoresis of linear DNA, where self-avoidance is usually neglected because of the two following reasons: first, according to the repton model, DNA crawls along tubes in the gel and it is in an elongated configuration where self-intersections are negligible. Secondly, it is often assumed that the drifting DNA can be considered to be in a semidilute solution regime, where polymers obey random walk statistics. Instead, in our case the conservation of the knot topology during the dynamics imposes the inclusion of self-avoidance.

CONCLUSION

In summary, we have presented a Monte Carlo simulation of gel electrophoresis of DNA knots. Our simulation reproduces the experimental findings (21,22), namely that complex knots migrate quicker than simple knots at low voltages, whereas at high voltages the behavior is inverted.

We thank A. Baldereschi, G. D'Anna, J. Roca, J. Schvartzman, J.-L.Viovy, and X. Zotos for help and for fruitful discussions.

This work was partially supported by the Swiss National Science Foundation (grants Nos. 21-50805.97, 200021-101851, 3100A0-103962 and 3152-68151).

REFERENCES

1. Noolandi, J., J. Rousseau, G. W. Slater, C. Turmel, and M. Lalande. 1987. Self-trapping and anomalous dispersion of DNA in electrophoresis. *Phys. Rev. Lett.* 58:2428–2431.
2. Deutsch, J. M. 1988. Theoretical studies of DNA during gel electrophoresis. *Science.* 240:922–924.
3. Viovy, J. L. 1988. Molecular mechanism of field-inversion electrophoresis. *Phys. Rev. Lett.* 60:855–858.
4. Doi, M., T. Kobayashi, Y. Makino, M. Ogawa, G. W. Slater, and J. Noolandi. 1988. Band inversion in gel electrophoresis of DNA. *Phys. Rev. Lett.* 61:1893–1896.
5. Noolandi, J., G. W. Slater, H. A. Lim, and J. L. Viovy. 1989. Generalized tube model of biased reptation for gel electrophoresis of DNA. *Science.* 243:1456–1458.
6. Duke, T. A., and J. L. Viovy. 1992. Simulation of megabase DNA undergoing gel electrophoresis. *Phys. Rev. Lett.* 68:542–545.
7. Aalberts, D. P. 1995. Electrophoretic mobility of asymmetric reptating polymers. *Phys. Rev. Lett.* 75:4544–4547.
8. Semenov, A. N., and J.-F. Joanny. 1997. Formation of hairpins and band broadening in gel electrophoresis of DNA. *Phys. Rev. E.* 55:789–799.
9. Schwartz, D. C., and M. Koval. 1989. Conformational dynamics of individual DNA molecules during gel electrophoresis. *Nature.* 338: 520–522.
10. Smith, S. B., P. K. Aldridge, and J. B. Callis. 1989. Observation of individual DNA molecules undergoing gel electrophoresis. *Science.* 243:203–206.
11. Sturm, J., and G. Weill. 1989. Direct observation of DNA chain orientation and relaxation by electric birefringence: Implications for the mechanism of separation during pulsed-field gel electrophoresis. *Phys. Rev. Lett.* 62:1484–1487.
12. Wang, Z., and B. Chu. 1989. Electrophoretic mobility and deformation of large DNA during gel electrophoresis. *Phys. Rev. Lett.* 63:2528–2531.
13. Dean, F. B., A. Stasiak, T. Koller, and N. R. Cozzarelli. 1985. Duplex DNA knots produced by *Escherichia coli* topoisomerase I. Structure and requirements for formation. *J. Biol. Chem.* 260:4975–4983.
14. Spengler, S. J., A. Stasiak, and N. R. Cozzarelli. 1985. The stereostructure of knots and catenanes produced by phage lambda integrative recombination: implications for mechanism and DNA structure. *Cell.* 42:325–334.
15. Duplantier, B., G. Jannink, and J. L. Sikorav. 1995. Anaphase chromatid motion: involvement of type II DNA topoisomerases. *Biophys. J.* 69:1596–1605.
16. Schvartzman, J. B., and A. Stasiak. 2004. A topological view of the replicon. *EMBO Rep.* 5:256–261.
17. Arsuaga, J., M. Vazquez, S. Trigueros, D. W. Sumners, and J. Roca. 2002. Knotting probability of DNA molecules confined in restricted volumes: DNA knotting in phage capsids. *Proc. Natl. Acad. Sci. USA.* 99:5373–5377.
18. Stasiak, A., V. Katritch, J. Bednar, D. Michoud, and J. Dubochet. 1996. Electrophoretic mobility of DNA knots. *Nature.* 384:122.
19. Garcia de la Torre, J. G., and V. A. Bloomfield. 1981. Hydrodynamic properties of complex, rigid, biological macromolecules: theory and applications. *Q. Rev. Biophys.* 14:81–139.
20. Vologodskii, A. V., N. J. Crisona, B. Laurie, P. Pieranski, V. Katritch, J. Dubochet, and A. Stasiak. 1998. Sedimentation and electrophoretic migration of DNA knots and catenanes. *J. Mol. Biol.* 278:1–3.
21. Trigueros, S., J. Arsuaga, M. E. Vazquez, D. W. Sumners, and J. Roca. 2001. Novel display of knotted DNA molecules by two-dimensional gel electrophoresis. *Nucleic Acids Res.* 29:E67.
22. Sogo, J. M., A. Stasiak, M. L. Martinez-Robles, D. B. Krimer, P. Hernandez, and J. B. Schvartzman. 1999. Formation of knots in partially replicated DNA molecules. *J. Mol. Biol.* 286:637–643.
23. Valle, F., M. Favre, J. Roca, and G. Dietler. 2005. Atomic force microscopy of complex DNA knots. *In* Physical and Numerical Models in Knot Theory, Vol. 36 of Series on Knots and Everything, Chapter 9. J. A. Calvo, K. C. Millett, E. J. Rawdon, and A. Stasiak, editors. World Scientific, Singapore, 161–170.
24. Socci, N. D., J. N. Onuchic, and P. G. Wolynes. 1999. Stretching lattice models of protein folding. *Proc. Natl. Acad. Sci. USA.* 96:2031–2035.
25. Marcone, B., E. Orlandini, and A. L. Stella. 2005. What is the length of a knot in a polymer? *J. Phys. A.-Math. Gen.* 38:L15–L21.
26. Caraciollo, S., M. S. Causo, and A. Pelissetto. 1998. High-precision determination of the critical exponent gamma for self-avoiding walks. *Phys Rev E.* 57:R1215–R1218.
27. Dobay, A., J. Dubochet, K. Millett, P.-E. Sottas, and A. Stasiak. 2003. Scaling behavior of random knots. *Proc. Natl. Acad. Sci. USA.* 100: 5611–5615.
28. Janse van Rensburg, E., E. Orlandini, D. Sumners, M. Tesi, and S. Whittington. 1997. The writhe of knots in the cubic lattice. *J. Knot Theor. Ramif.* 6:31–44.
29. Katritch, V., J. Bednar, D. Michoud, R. Scharein, J. Dubochet, and A. Stasiak. 1996. Geometry and physics of knots. *Nature.* 384:142–145.
30. Berg, B., and D. Foerster. 1981. Random paths and random surfaces on a digital computer. *Phys. Lett. B.* 106:323–326.
31. Aragão de Carvalho, C., S. Caracciolo, and J. Fröhlich. 1983. Polymers and $g\,|\phi|^4$ theory in four dimensions. *Nucl. Phys. B.* 215:209–248.
32. Lim, H. A. 1996. Electrophoresis of topologically nontrivial macromolecules: mathematical and computational studies. *Int. J. Mod. Phys. C.* 7:217–271.
33. Janse van Rensburg, E., and S. Whittington. 1991. The dimensions of knotted polygons. *J. Phys. A.* 24:3935–3948.
34. Alexander, J. W. 1928. Topological invariants of knots and links. *Trans. Am. Math. Soc.* 30:275–306.
35. Viovy, J. 2000. Electrophoresis of DNA and other polyelectrolytes: physical mechanisms. *Rev. Mod. Phys.* 72:813–872.
36. van Heukelum, A., and G. T. Barkema. 2002. Lattice models of DNA electrophoresis. *Electrophoresis.* 23:2562–2568.